2006-05-01

Design of compact polymer Mach-Zender interferometer and ring resonator with air trench structures

Seunghyun Kim
University of Alabama in Huntsville, shkim@eng.uah.edu

Jianhua Jiang

Gregory P. Nordin
Brigham Young University - Provo, nordin@byu.edu

Original Publication Citation

Seunghyun Kim, Jianhua Jiang, and Gregory P. Nordin, Design of compact polymer Mach-Zender interferometer and ring resonator with air trench structures, Opt. Eng. 45, 5462 (26)

Design of compact ring resonator and Mach-Zehnder interferometer with air trenches

Seunghyun Kim
Jianhua Jiang
Gregory P. Nordin, MEMBER SPIE
University of Alabama in Huntsville
Nano and Micro Devices Center
OB 418
Huntsville, Alabama 35899
E-mail: shkim@eng.uah.edu

Abstract. We discuss the design of a compact ring resonator (RR) and Mach-Zehnder interferometer (MZI) in a low-refractive-index-contrast waveguide material system through the use of air trenches. A narrow air trench at the intersection of one input and two output waveguides can function as a high-efficiency splitter, while wider air trenches operate as waveguide bends. We first discuss the design of individual splitters and bends and then show how they can be used to realize a compact MZI and RR. The RR has a footprint of only 70×100 μm, and its optical efficiency at the drop wavelengths is $\approx$86%. The free spectral range and full width at half maximum are 7.2 and 0.5 nm, while the Q factor is $>$3,000. The MZI occupies only 165×130 μm, and its calculated optical efficiency is 90%. © *2006 The Society of Photo-Optical Instrumentation Engineers.* [DOI: 10.1117/1.2202926]

Subject terms: planar lightwave circuit; air trenches; ring resonator; Mach-Zehnder interferometer; total internal reflection; integrated optics; guided waves; integrated optics devices.

Paper 050657R received Aug. 17, 2005; revised manuscript received Sep. 8, 2005; accepted for publication Sep. 9, 2005; published online May 23, 2006. This paper is a revision of a paper presented at the SPIE conference on Optoelectronic Integrated Circuits VII, Jan. 2005, San Jose, California. The paper presented there appears in SPIE Proceedings Vol. 5729.

1 Introduction

Ring resonators (RRs) and Mach-Zehnder interferometers (MZIs) are fundamental building blocks for a variety of applications, including add-drop and bandpass filters, wavelength division multiplexer/demultiplexers, and all optical switches.[1–7] Low index contrast (LIC) waveguide materials, such as silica and many polymers, are attractive for planar lightwave circuits (PLCs) because of their low propagation loss, low coupling loss to and from fibers, and mature microfabrication processes.[1–3,8] However, since the radius of curvature required for high-efficiency LIC waveguide bends is large (on the order of millimeters to centimeters),[9,10] compact RRs and MZIs have not been realized with conventional LIC waveguides.

In this paper, we present designs for a compact, high-efficiency RR and MZI for a polymer waveguide material system. We first show how small-area splitters can be realized with air trenches. A narrow air trench at the intersection of an input and two output waveguides operates as a high-efficiency beamsplitter through frustrated total internal reflection (FTIR). Combined with appropriate air-trench bends,[11,12] we design a RR and MZI and discuss their performance based on simulation results. For the purpose of this paper, we limit our analysis to TM polarization (operation with TE polarization requires a simple redesign of the structures to adjust air trench positions and widths). We use a two-dimensional (2-D) finite-difference time-domain (FDTD) method[13] with Berenger perfectly matched layer (PML) boundary conditions[14] to numerically simulate the designed structures. A three-dimensional (3-D) FDTD method is used to verify the 2-D FDTD results.

2 Splitters with Air Trenches

We consider a perfluorcyclobutyl (PFCB)[15,16] channel waveguide structure with core and cladding refractive indices of 1.4816 and 1.4625, respectively. For single-mode operation at a wavelength of 1.55 μm, the waveguide core is chosen to be 3.6×3.6 μm. For 2-D FDTD calculations, we use the effective-index method[17] to approximate this as a 2-D structure with a waveguide width of 3.6 μm and a core refractive index of 1.4755. The cladding index remains the same.

To realize a splitter, an air trench is positioned as shown in Fig. 1(a). We first calculate optical efficiencies at output waveguide channels 1 and 2 as a function of the air-trench width. For a waveguide mode incident along the input waveguide, optical efficiencies have been calculated at output channels 1 and 2 with a mode overlap integral (MOI) (i.e., the optical efficiency is defined as the ratio of the power in the guided mode at the output detector to that in the incident guided mode).[18] The result is shown in Fig. 1(b). As seen in the figure, the splitting ratio is about 50:50 with an air-trench width of 0.42 μm. As the air-trench width increases, the optical efficiency in channel 2 increases while the optical efficiency in channel 1 correspondingly decreases.

For a ring resonator, we choose a 0.8-μm-wide air trench, for which we have already demonstrated fabrication feasibility with etch depth in the 14- to 16-μm range.[19] Figure 2(a) shows the time-averaged magnitude squared of the electric field at $\lambda=1.55$ μm. The optical efficiencies

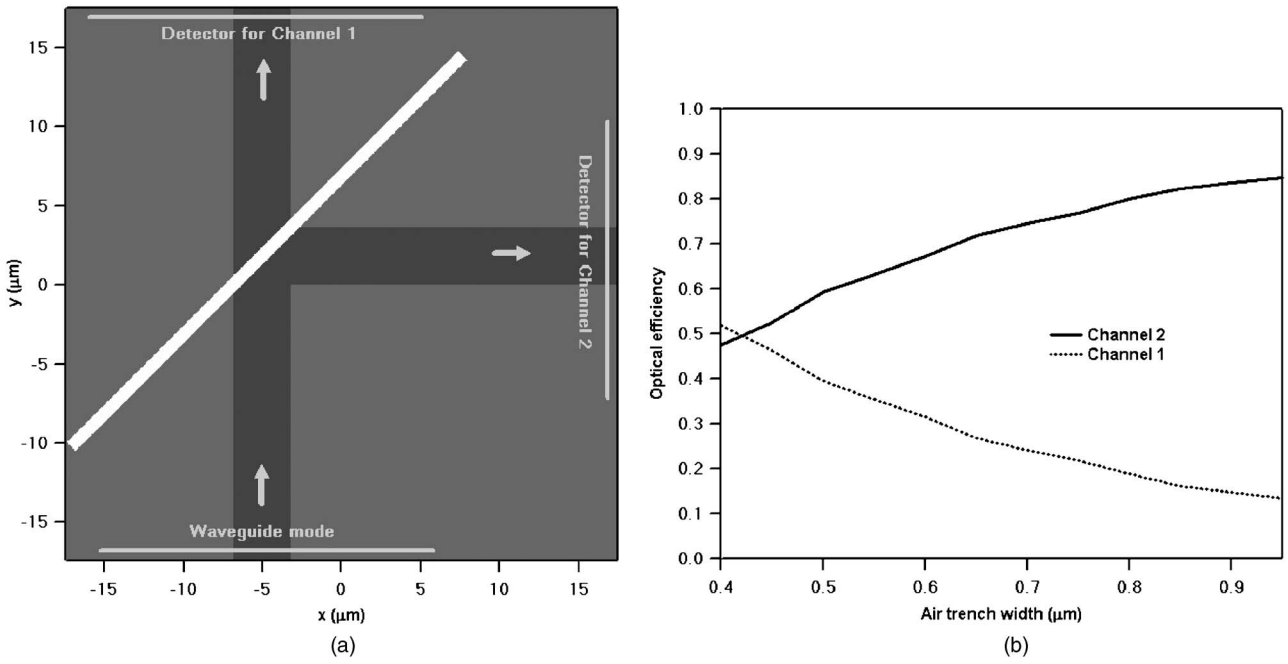

Fig. 1 (a) Geometry of splitter design with an air trench. (b) Optical efficiencies at output waveguide channels 1 and 2 as a function of air-trench width. A 50:50 splitting ratio is achieved with 0.42-μm air-trench width.

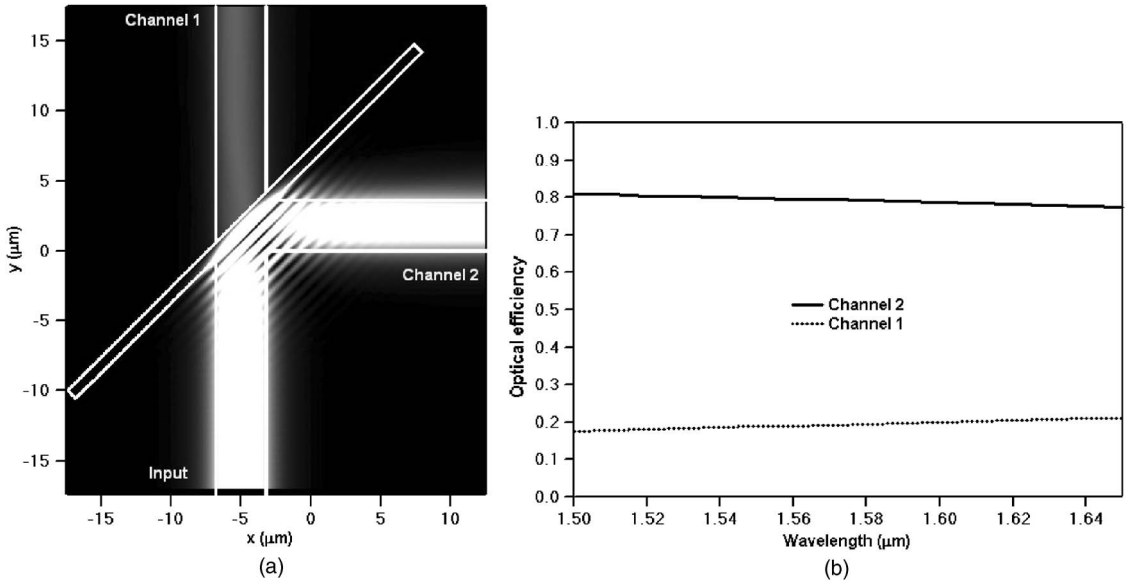

Fig. 2 (a) Time-averaged magnitude squared of the electric field of a splitter design for a ring resonator at $\lambda = 1.55$ μm. Air-trench width is 0.8 μm. (b) Spectral response of the splitter design.

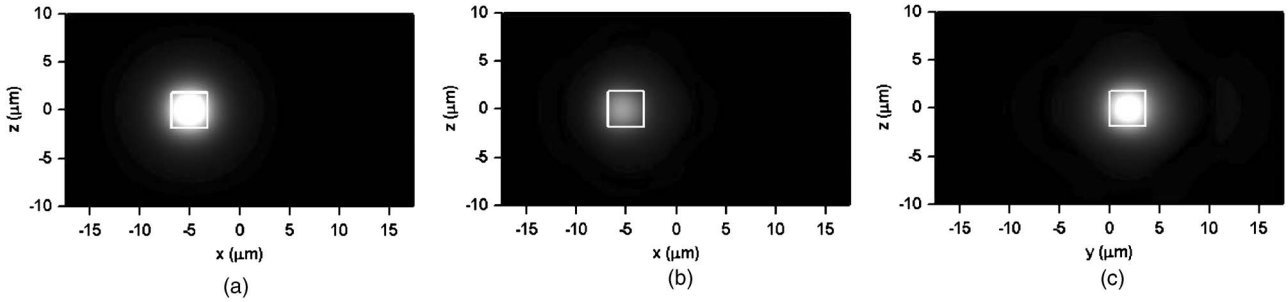

Fig. 3 (a) Input waveguide mode for 3-D FDTD method. Electric field at detectors in output channels (b) 1 and (c) 2.

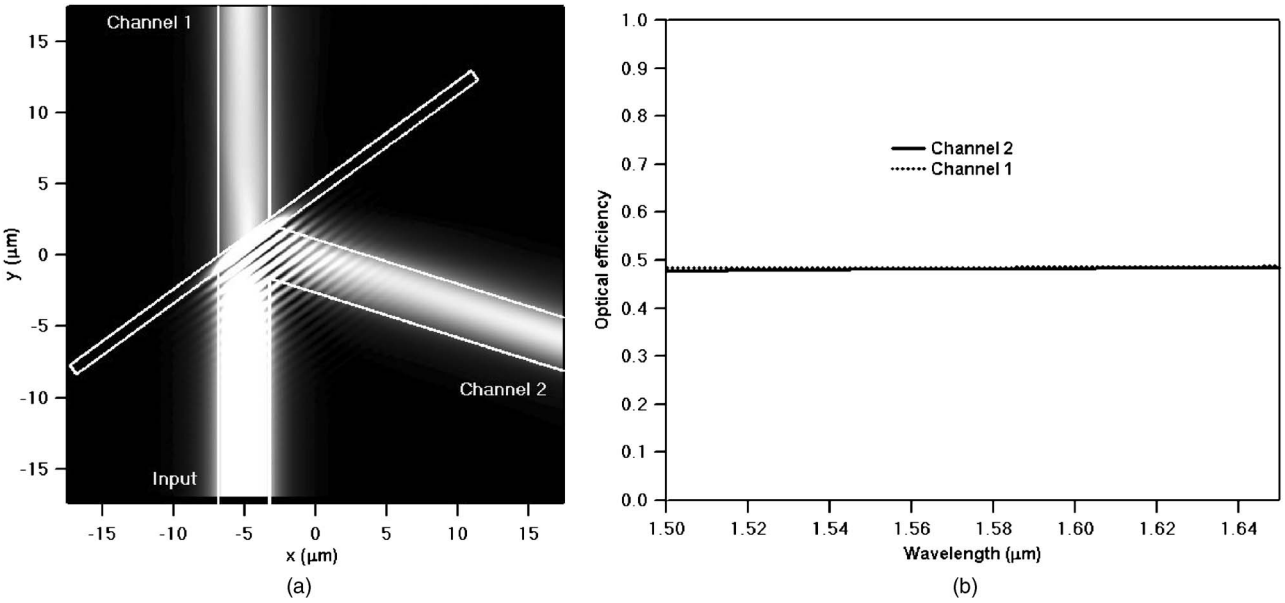

Fig. 4 (a) Time-averaged magnitude squared of the electric field of a splitter for a Mach-Zehnder interferometer at $\lambda = 1.55$ μm. The air-trench width is 0.8 μm, and the angle between channels 1 and 2 is 107.5 deg. (b) Spectral response of the splitter.

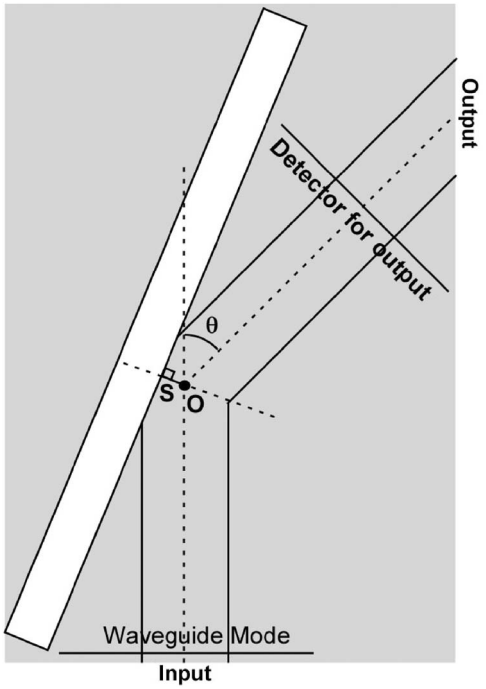

Fig. 5 Geometry of a waveguide bend with an air trench. The position of the incident waveguide mode source is shown, as well as the detector position along the output waveguide.

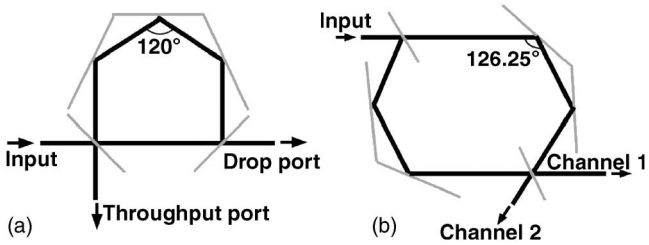

Fig. 6 Proposed (a) ring resonator and (b) Mach-Zehnder interferometer using small-area air-trench bends and splitters.

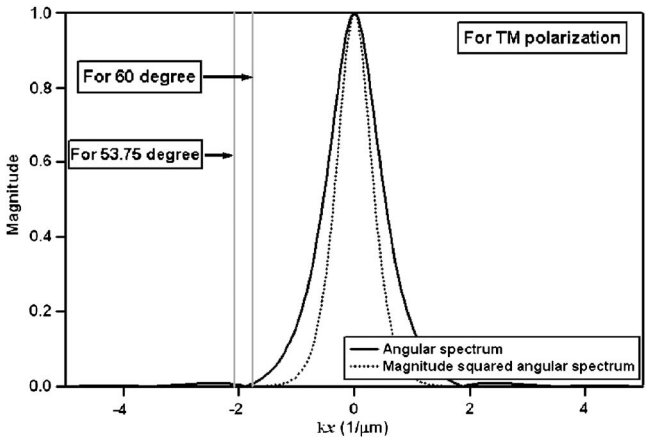

Fig. 7 Angular spectrum of the waveguide mode. The two vertical lines correspond to plane-wave components at the critical angles for 60- and 53.75-deg bend structures.

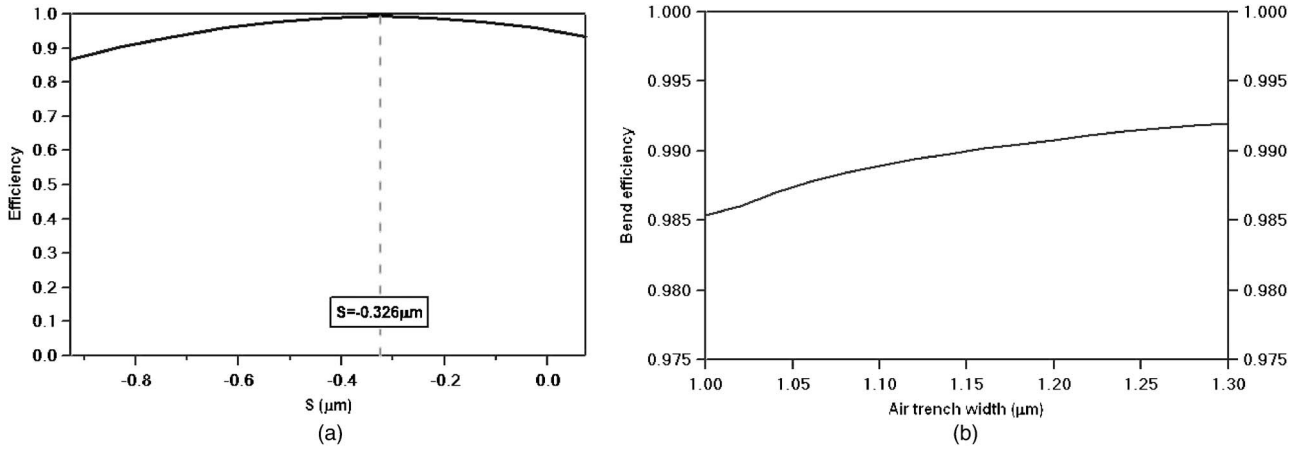

Fig. 8 (a) Bend efficiency as a function of *S*. Bend efficiency at $S=-0.326$ μm is 99.3%. (b) Bend efficiency as a function of air-trench width.

calculated with 2-D FDTD at channels 1 and 2 are 18.8% and 79.9% (total 98.7%), respectively. The spectral response of the splitter is shown in Fig. 2(b). Note that the wavelength dependence is quite small, as expected.

We employ 3-D FDTD to verify the 2-D FDTD results. The waveguide source for 3-D FDTD is shown in Fig. 3(a) while Figs. 3(b) and 3(c) show magnitude of the TM electric field component at detectors in the output channels. The optical efficiencies calculated by 3-D FDTD (with MOI) are 19.1% (channel 1) and 78.3% (channel 2), which are matched very well with the 2-D FDTD results.

The splitting ratio of a splitter for a MZI should be 50:50. As noted, the air-trench width must be 0.42 μm for the 90-deg splitter geometry. However, this is correspondingly more difficult to fabricate because of the large etch aspect ratio. Instead, we change the bend angle of channel 2 while keeping the air-trench width at 0.8 μm until the splitting ratio is essentially 50:50. The final design is shown in Fig. 4(a) for $\lambda=1.55$ μm. The angle between channels 1 and 2 is 107.5 deg, and the optical efficiencies are 48.5% and 48.1%, respectively. Figure 4(b) shows the spectral response of the splitter. The splitting ratio is essentially uniform over the wavelength range shown in the figure (1.50 to 1.65 μm).

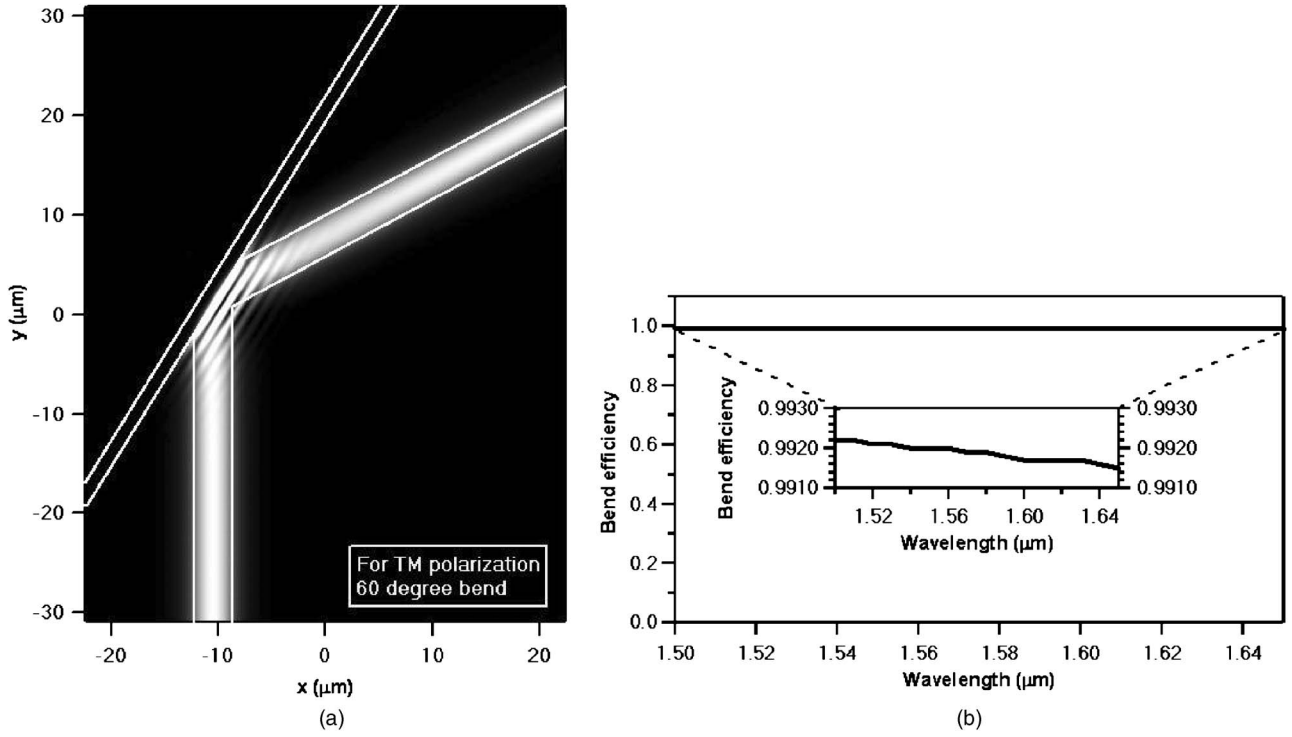

Fig. 9 (a) Geometry and time-averaged magnitude squared of the electric field of the final 60-deg bend design at $\lambda=1.55$ μm. (b) Spectral response.

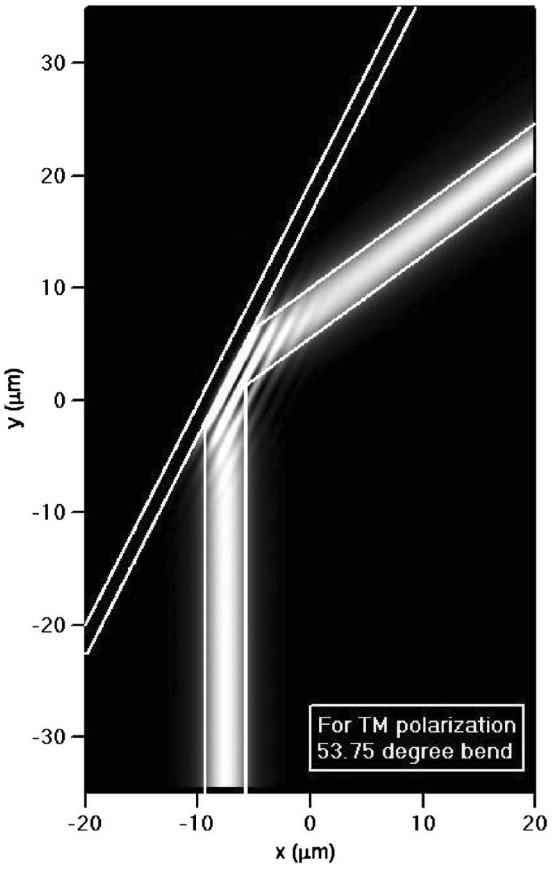

Fig. 10 Geometry and time-averaged magnitude squared of the electric field of the final 53.75-deg bend design at $\lambda = 1.55$ μm.

3 Bends with Air Trenches

High-efficiency small-area waveguide bends for RR and MZI are also designed with air trenches.[11,12] Before we discuss waveguide bends, we need to define the bend angle and terms used for the waveguide-bend design. The geometry of a bend structure is shown in Fig. 5. The angle between the bisecting lines of the input and output waveguides is defined as the bend angle θ. The intersection of the bisecting lines of the input and output waveguides is the origin O, and the distance from the origin to the air-trench interface is defined as the separation S, which is measured along a line orthogonal to the air-trench interface and intersecting O. It is positive when the air-trench interface moves away from the bend, and negative when it moves past O into the bend. Because of the Goos-Hanschen shift at the air interface, the value for S that gives the highest optical efficiency is always negative.

As discussed in detail in Ref. 12, high bend efficiency can be achieved when the waveguide mode is incident on the air-trench interface at an angle such that all of the plane-wave components of the mode undergo TIR. For waveguide material systems in which the core and cladding refractive indices are low, bend angles less than 90 deg are generally needed. As shown in Fig. 6, we therefore choose RR and MZI bend angles of 60 and 53.75 deg, respectively, in order to both meet this constraint and have symmetric device configurations. Figure 7 shows the angular spectrum of the waveguide mode, with vertical lines corresponding to plane-wave components at the critical angles for 60- and 53.75-deg bends. Plane-wave components to the right of each vertical line satisfy the TIR condition for that particular bend. We clearly can expect high bend efficiency for both bend angles.

To design the bend structures, we first find the optimum position of the air-trench interfaces and then choose an adequate width for the air trench. We first consider the 60-deg bend for a ring resonator. Figure 8(a) shows the bend efficiency as a function of S at a wavelength of 1.55 μm. The bend efficiency has a maximum of 99.3% at $S = -0.326$ μm. Keeping the air-trench interface at this position, the bend efficiency as a function of the air trench width is shown in Fig. 8(b). As the width increases, the amount of optical power transmitted through the air trench by FTIR decreases exponentially. To minimize aspect-ratio-dependent etch effects (i.e., different etch depths for different trench widths) between bends and splitters during the fabrication process, the air-trench width of a bend should

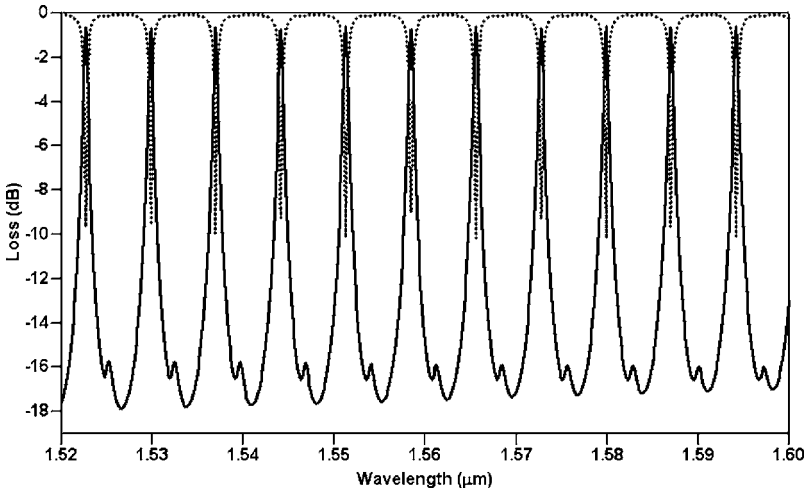

Fig. 11 Ring-resonator spectral response.

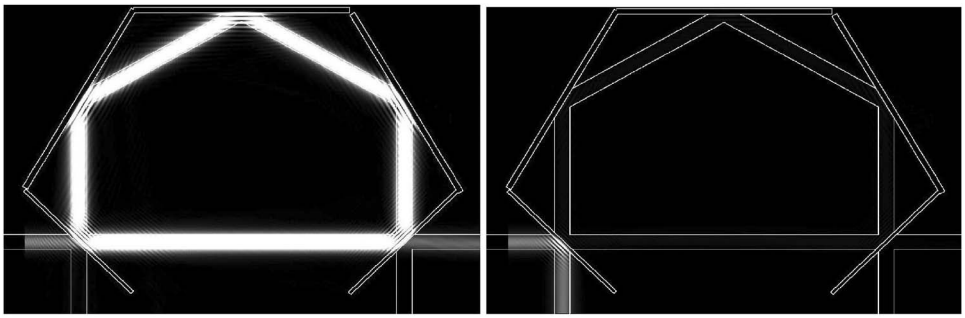

Fig. 12 Time-averaged magnitude squared of the electric field at (a) $\lambda = 1.5513\ \mu$m (one of the drop wavelengths) and (b) $\lambda = 1.5549\ \mu$m (one of the throughput wavelengths).

not be too different from that of the splitter (0.8 μm). We therefore choose an air-trench width of 1.3 μm. In this case, the bend efficiency is 99.2%.

The geometry of the final 60-deg bend design is shown in Fig. 9(a) along with the time-averaged magnitude squared of the electric field for $\lambda = 1.55\ \mu$m. Figure 9(b) shows the spectral response of the bend for a wavelength range of 1.50 to 1.65 μm. This design has also been verified with 3-D FDTD, in which the bend efficiency at $\lambda = 1.55\ \mu$m is 98.9%, which is consistent with the 2-D FDTD result.

For the MZI, we designed a 53.75-deg waveguide bend structure by following the same process as described for the 60-deg bend. In this case, the bend efficiency is maximized for $S = -0.254\ \mu$m. The width of the air trench is chosen as 1.3 μm. Figure 10 shows the time averaged magnitude squared of the electric field at $\lambda = 1.55\ \mu$m. The calculated bend efficiency is 99.1%.

4 Compact Ring Resonator and Mach-Zehnder Interferometer

The final RR design shown in Fig. 6(a) occupies an area of only $70 \times 100\ \mu$m. The simulated performance using 2-D FDTD is shown in Fig. 11. The solid and dotted lines are the optical efficiencies at the drop and throughput ports, respectively. The optical efficiency at the drop wavelengths (i.e., wavelengths at which most of the light exits through the drop port) is 86%. The free spectral range (FSR) is 7.2 nm, and the full width at half maximum (FWHM) is 0.5 nm. The Q factor is >3000. Figure 12 shows the time-averaged magnitude squared of the electric field at $\lambda = 1.5513\ \mu$m (one of the drop wavelengths) and $\lambda = 1.5549\ \mu$m (one of the throughput wavelengths).

With 53.75-deg bends and 107.5-deg splitters, the MZI occupies only $165 \times 130\ \mu$m. The time-averaged magnitude squared of the electric field at $\lambda = 1.55\ \mu$m is shown in Fig. 13. The optical efficiency along channel 1 is 90.2%.

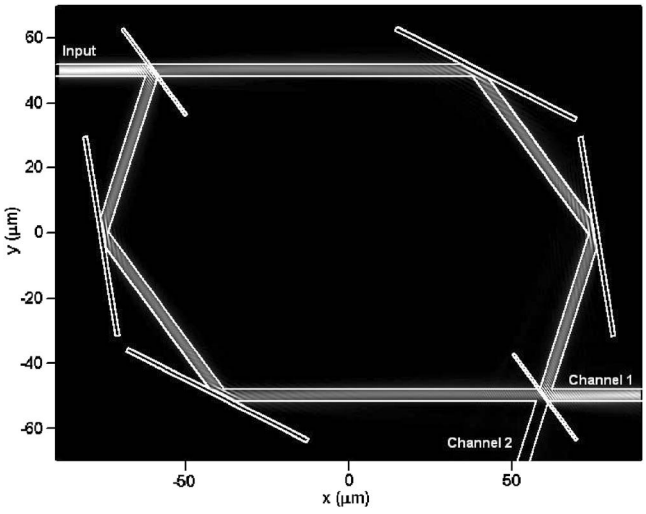

Fig. 13 Time-averaged magnitude squared of the electric field of the compact MZI at $\lambda = 1.55\ \mu$m.

5 Conclusion

Air trenches can be used to realize both small-area bends and splitters, which in turn enables the design of very compact RRs and MZIs. We have illustrated this approach for a low-index waveguide material system. 2-D FDTD is used for the main design work, and 3-D FDTD is used to validate the 2-D FDTD results. We are now developing the fabrication process required to realize these devices physically and compare experimental results with simulations.

Acknowledgment

This work was supported in part by DARPA grant N66001–04–8933 and National Science Foundation grant EPS-0091853.

References

1. P. Rabiei, W. H. Steier, C. Zhang, and L. R. Dalton, "Polymer microring filters and modulators," *J. Lightwave Technol.* **20**(11), 1968–1975 (2002).
2. W.-Y. Chen, R. Grover, T. A. Ibrahim, V. Van, W. N. Herman, and P.-T. Ho, "High-finesse laterally coupled single-mode benzocyclobutene microring resonators," *IEEE Photonics Technol. Lett.* **16**(2), 470–472 (2004).
3. L. Zuo, H. Suzuki, K. Kong, J. Si, M. M. Aye, A. Watabe, and S. Takahashi, "Athermal silica-based interferometer-type planar lightwave circuits realized by a multicore fabrication method," *Opt. Lett.* **28**(12), 1046–1048 (2003).
4. W. M. J. Green, R. K. Lee, G. A. DeRose, A. Scherer, and A. Yariv, "Hybrid InGaAsP-InP Mach-Zehnder racetrack resonator for thermooptic switching and coupling control," *Opt. Express* **13**(5), 1651–1659 (2005).
5. T. P. White, C. M. de Sterke, R. C. McPhedran, T. Huang, and L. C. Botten, "Recirculation-enhanced switching in photonic crystal Mach-Zehnder interferometers," *Opt. Express* **12**(13), 3035–3045 (2004).
6. I. Kiyat, A. Aydinli, and N. Dagli, "High-Q silicon-on-insulator op-

tical rib waveguide racetrack resonators," *Opt. Express* **13**(6), 1900–1905 (2005).
7. A. Vorckel, M. Monster, W. Henschel, P. H. Bolivar, and H. Kurz, "Asymmetrically coupled silicon-on-insulator microring resonators for compact add-drop multiplexers," *IEEE Photonics Technol. Lett.* **15**(7), 921–923 (2003).
8. A. Yeniay, R. Gao, K. Takayama, R. Gao, and A. F. Garito, "Ultra-low-loss polymer waveguides," *J. Lightwave Technol.* **22**(1), 154–158 (2004).
9. D. L. Lee, *Electromagnetic Principles of Integrated Optics*, John Wiley & Sons, New York (1986).
10. C. T. Lee and M. L. Wu, "Apexes-linked circle gratings for low-loss waveguide bends," *IEEE Photonics Technol. Lett.* **13**(6), 597–599 (2001).
11. L. Li, G. P. Nordin, J. M. English, and J. Jiang, "Small-area bends and beamsplitters for low-index-contrast waveguides," *Opt. Express* **11**(3), 282–290 (2003).
12. J. Cardenas, L. Li, S. Kim, and G. P. Nordin, "Compact low loss single air interface bends in polymer waveguides," *Opt. Express* **12**(22), 5314–5324 (2004).
13. A. Taflove, *Computational Electrodynamics: The Finite-Difference Time-Domain Method*, Artech House, Boston (1995).
14. J. P. Berenger, "A perfectly matched layer for the absorption of electromagnetic waves," *J. Comput. Phys.* **114**(2), 185–200 (1994).
15. D. W. Smith, Jr., S. Chen, S. Kumar, J. Ballato, H. Shah, C. Topping, and S. H. Foulger, "Perfluorocyclobutyl copolymers for microphotonics," *Adv. Mater. (Weinheim, Ger.)* **14**(21), 1585–1589 (2002).
16. D. W. Smith, Jr., A. B. Hoeglund, H. V. Shah, M. J. Radler, and C. A. Langhoff, "Perfluorocyclobutane polymers for optical fibers and dielectric waveguides," Chap. 4 in *Optical Polymers*, J. Harmon, Ed., ACS Symp. Ser. vol.795, pp. 49–62 (2001).
17. H. Nishihara, M. Haruna, and T. Suhara, *Optical Integrated Circuits*, Chap. 2, pp. 31–32, McGraw-Hill, New York (1989).
18. R. R. A. Syms and J. Cozens, *Optical Guided Waves and Devices*, Chap. 6, pp. 120–144, McGraw-Hill, New York (1992).
19. G. Nordin, J. Cardenas, and S. Kim, "Compact high efficiency bends in perfluorocyclobutyl polymer waveguides" in *OFC 2005*, Opt. Soc. Am. (2005).

Seunghyun Kim is a research scientist of the Nano and Micro Devices Center at the University of Alabama in Huntsville. He received his BS degree in physics from the Suwon University, Republic of Korea, in 1998, and his PhD degree in optical science and engineering from the University of Alabama in Huntsville, USA, in 2004. His researches are focused on design and fabrication of integrated planar photonic devices and photonics-based chemical and biological sensors.

Jianhua Jiang is employed as a research scientist by the Nano and Micro Devices Center (NMDC) at the University of Alabama in Huntsville (UAH). He received his undergraduate degree in physics and master's in optics from Tsinghua University, Beijing, China, in 1993 and 1996, respectively. In 2000, he earned his doctorate from the University of Alabama in Huntsville in optical science and engineering. His research interests are rigorous grating theory and numerical modeling methods for photonic devices.

Gregory P. Nordin is the director of the Nano and Micro Devices Center and a professor in the Department of Electrical and Computer Engineering at the University of Alabama in Huntsville. He received his PhD degree from the University of Southern California in 1992. His current research activities include photonic devices for high-density planar lightwave circuit integration, MEMS and photonics-based chemical and biological sensors, nano and micro fabrication, and microfluidic devices.